Journal of Applied Polymer Science

Influence of a Sorbitol-Based Nucleating Agent Modified with Silsesquioxanes on the Non-Isothermal Crystallization of Isotactic Polypropylene

Mateusz Barczewski,[1] Monika Dobrzyńska-Mizera,[1] Beata Dudziec,[2] Tomasz Sterzyński[1]

[1]Polymer Processing Division, Poznań University of Technology, Institute of Materials Technology, Piotrowo 3, 61-138 Poznań, Poland

[2]Department of Organometallic Chemistry, Adam Mickiewicz University, Faculty of Chemistry, Grunwaldzka 6, 60-780 Poznań, Poland

Correspondence to: M. Barczewski (E-mail: mateusz.barczewski@put.poznan.pl)

ABSTRACT: This article investigates the effect of modifying the polypropylene (iPP) α-phase nucleating agent 1,3:2,4-bis(3,4-dimethylbenzylidene) sorbitol (DMDBS) with tetrasilanolphenyl silsesquioxane (phPOSS). It has been proven that an increasing amount of silsesquioxane leads to differences in the crystallization behavior. What is more, it has been observed that the nucleation effect that results from the addition of sorbitol derivatives is suppressed by phPOSS activity. To understand the influence of phPOSS addition on the crystallization kinetics of PP/DMDBS/phPOSS composites that have been prepared by melt processing in a twin screw extruder, differential scanning calorimetry, rotational rheometry and Fourier transform infrared spectroscopy are performed.
 J. Appl. Polym. Sci. **2014**, *131*, 40131.

KEYWORDS: polyolefins; rheology; crystallization; nanoparticles; nanowires and nanocrystals; nanostructured polymers

Received 17 May 2013; accepted 23 October 2013
DOI: 10.1002/app.40131

INTRODUCTION

Isotactic polypropylene (iPP) composites that were modified with polyhedral oligomeric silsesquioxanes have been widely studied. Specifically, the effect of incorporating silsesquioxanes into the polymeric matrix on the composite's properties, such as the rheological behavior, thermal stability, oxidation resistance, surface modification, crystallization, structure, and mechanical properties, has been investigated.[1–11] It was shown that the effects of modifying thermoplastic polymers with only silsesquioxanes using a non-reactive mixing process in a molten state are typically insufficient to change the properties of iPP significantly,[12–14] which is the main reason why grafting silsesquioxanes with modifying agents to improve their modification efficiency is receiving considerable attention in many contemporary works.[15–20]

The high efficiency and relatively low cost of sorbitol derivatives make them one of the most widely used nucleating agents. Their applicability is limited by the crystallization of iPP, which occurs during the production of highly oriented films with high transparency due to the addition of a nucleating agent. Thus, a high level of orientation may not be achieved, and an increase in the viscosity of the polymer melt is typically observed. The modification effect that is caused by the inclusion of sorbitol-based nucleating agents to achieve a high draw ratio during PP fiber spinning was investigated by Roy et al. and is presented in several papers.[18,19]

Two different silsesquioxane types, with various properties to describe their behaviors in a polymer melt, will be discussed. The first type, called compatible or nonreactive, includes silsesquioxanes that are easily distributed in a polymer melt using standard melt mixing devices, such as a twin-screw extruder or periodic kneader. It is known that nonreactive silsesquioxane molecules do not covalently bond to a polymer matrix and that the dispersion depends on the character of the side groups of POSS.[1] The second group of silsesquioxanes is called incompatible or reactive and includes nanomodifiers and fillers that typically exhibit significant difficulty in achieving a uniform distribution in a polymeric matrix. In this case, particle agglomerates form due to the strong chemical bonds that are observed between the POSS particles.[20]

The mechanism of hydrogen bond creation between silanol-POSS and DMDBS has been described in a number of papers.[18–20] Roy et al. obtained fibers with significantly improved mechanical properties via the addition of siloxanes that contained different phenyl reactive groups to iPP that was

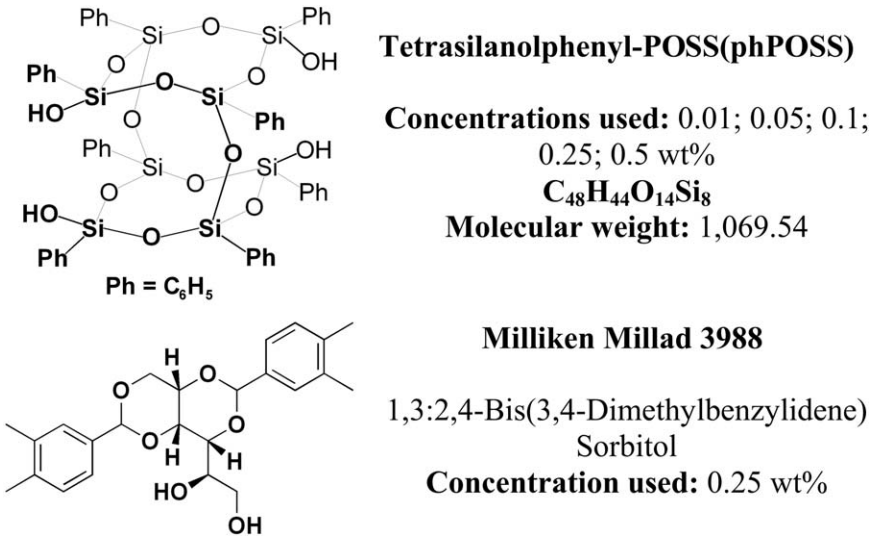

Figure 1. Modifier and nucleating agent used in our studies.

nucleated by (1,3:2,4)dibenzylidene sorbitol (DBS). Comprehensive research led to a description of the interactions between the two aforementioned groups of additives. Note that in all of the papers, the amount of modifiers and nucleating agents is relatively high, which may result in their exclusion from industrial applications; from this perspective, the use of expensive silsesquioxanes may lead to a limitation in their commercial application if the amount exceeds, for example, 0.5 wt %.[21–24]

The aim of this study is to describe how to modify DMDBS with phPOSS on account of a possibility of a viscosity increase control in iPP blends. The controlled crystallization can be used in the production of molten state highly oriented products due to extended processing time.

EXPERIMENTAL

Material

The commercial iPP Moplen HP500N, with MFR = 10 g/10 min (230°C, 2.16 kg) from Basell Orlen Polyolefins (Poland) was used in our experiments. The selected polymeric matrix is characterized by a low modification level.

The nucleating agent that was used in these studies was 1,3:2,4-bis(3,4-dimethylbenzylidene) sorbitol, Millad 3988l (DMDBS), which is a third-generation sorbitol derivative that is offered by the Milliken Chemical Company (USA). Tetrasilanolphenyl-POSS ($C_{44}H_{44}O_{14}Si_8$), abbreviated phPOSS, which acts as a modifier for the nucleating agent, was synthesized by the Department of Organometallic Chemistry UAM (Poznań, Poland). The thermal stability of all materials was determined using thermogravimetry (TGA), which enabled the confirmation of the usability of these materials at temperatures that are typically applied in the processing of iPP. The chemical formulas of the nucleating agent and modifier used in our studies are presented in Figure 1.

Preparation of phPOSS

All syntheses and manipulations were conducted under argon using standard Schlenk-line and vacuum techniques. ^1H, ^{29}Si NMR spectra were recorded on Bruker Avance 400 and 500 MHz in benzene-d_6 and $CDCl_3$. The Fourier transform infrared (FTIR) spectra were recorded on a Bruker Tensor 27 Fourier transform spectrophotometer equipped with a SPECAC Golden Gate diamond ATR unit. For all cases, 16 scans with a resolution of 2 cm^{-1} were collected to obtain the spectra.

Chemical products, such as $PhSi(OMe)_3$, 2-propanol, sodium hydroxide, butyl acetate, acetic acid, acetone, sodium hydrogen carbonate and anhydrous magnesium sulfate, were obtained from Aldrich. All solvents and liquid reagents were dried and distilled under argon prior to use.

Tetrasilanol Form of Double-Decker Phenylsilsesqioxane

The structure and synthetic route of the tetrasilanol form of double-decker phenylsilsesqioxane is shown in the scheme below (Figure 2), in which the following original procedures were applied[25,26]:

Sample Preparation. iPP pellets were milled into a powder in a Tria high-speed grinder. Before processing, both the nucleation agent and modifier were dried in vacuum for 2 h at a temperature of 120°C. The polymer was mixed with DMDBS and phPOSS in the rotary mixer Retsch GM 200 for 3 min at a rotation speed of 3000 rpm. The homogenization of the premixed blends with different phPOSS contents (0.01–0.5 wt %) and with a fixed DMDBS concentration of 0.25 wt % was assured by molten state extrusion with a Zamak corotating twin screw extruder operated at 190°C and 70 rpm. The screws were configured to process polyolefins, and the extruded rod was pelletized in a water bath. The samples for WAXS measurements were prepared in a form of moldings obtained by compression molding at a constant temperature of 200°C for 5 min. Then the formed samples were cooled down to a room temperature at rate of 10°C min^{-1}.

Measurements. To verify the influence of the DMDBS modification with phPOSS on the structure of the polymeric matrix, investigations were conducted on the morphology and

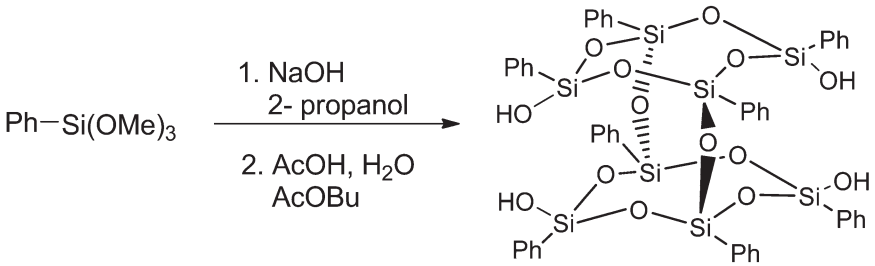

Figure 2. The structure and synthetic route of the tetrasilanol form of double-decker phenylsilsesqioxane.

rheological behavior during the crystallization of iPP using DSC, rotational rheometry and FTIR spectroscopy.

Differential Scanning Calorimetry (DSC). DSC was performed using a Netzsch DSC 204 F1 Phoenix® with aluminum crucibles and ~5 mg samples under a nitrogen flow. All of the samples were heated to 220°C and held in a molten state for 5 min, followed by cooling to 60°C at various cooling rates of $\phi = 5$, 10, 20, and 30°C min^{-1} to gain broad information on the crystallization process.[27]

The Avrami theory that was modified by Jeziorny has been used to analyze nonisothermal crystallization kinetics.[27–39] The Avrami equation was used in the following form:

$$1 - X_t = \exp\left(-Z_t t^n\right) \tag{1}$$

where Z_t is the Avrami constant rate, n is the Avrami exponent and X_t is the relative crystallinity at temperature T, which can be defined by

$$X_t = \frac{\int_0^t (dH(t)/dt)dt}{\int_0^\infty (dH(t)/dt)dt} \tag{2}$$

where $(dH(t)/dt)$ is the heat flow and $X_t(t)$ and $X_t(\infty)$ indicate the absolute crystallinity at time t and at the end of the crystallization process. By taking the double logarithm of eq. (1), the equation can be presented as

$$\ln\left[-\ln\left(1 - X_t\right)\right] = \ln Z_t + n \ln t \tag{3}$$

The relation between X_t and t that is expressed in the Avrami equation should be converted from temperature into time, which can be achieved using the following expression:

$$t = (T_0 - T)/\phi \tag{4}$$

where T is the temperature at time t, T_0 is the initial temperature (at the moment when crystallization starts) and ϕ is the cooling rate.

On the basis of the nonisothermal nature of the crystallization process, Jeziorny[29,31] found that the Avrami constant rate Z_t should include the cooling rate ϕ. Taking this fact into account, the final form of the equation that characterizes the kinetics of nonisothermal crystallization is

$$\ln Z_c = \ln Z_t/\phi \tag{5}$$

According to the literature,[27] it is possible to calculate the half crystallization time $t_{1/2}$ by applying the following eq. (6):

$$t_{1/2} = \left[\frac{\ln 2}{Z_t}\right]^{1/n} \tag{6}$$

The crystallinity degree was calculated from thermograms recorded during the second heating. The crystallinity degree ($X_{C\text{-}DSC}$) was evaluated on the basis of the melting heat (ΔH_m) during crystallization at a cooling rate of $\phi = 10$°C min^{-1}. The crystallinity degree of pure, nucleated and phPOSS modified samples was calculated using the following eq. (7):

$$X_c = \frac{\Delta H_M}{\Delta H_0} \times 100\% \tag{7}$$

where ΔH_o is the melting heat of entirely crystallized iPP and its value is equal to 207.1 J g^{-1}.[40]

Fourier Transform Infrared Spectroscopy (FTIR). The IR spectra were collected with a Bruker Vertex 70 FTIR spectrometer in absorption mode using 64 scans. The spectra resolution was 1 cm^{-1}. Sample specimens were prepared by mixing phPOSS and DMDBS with milled potassium bromide (KBr). This powder was then compressed in vacuum into thin pellets using a pressure of 20 MPa. Five different mixtures were examined. The first and second samples were prepared at ambient temperature using pure phPOSS and DMDBS, respectively. The other specimens were mixtures of phPOSS and DMDBS with a ratio of 1 : 1. For the tests, one sample was kept at ambient temperature, the second was heated to 190°C and the third reached a maximum temperature of 287°C. The spectra that were obtained during the measurements were stored and used for further analysis. All of the spectra were submitted to a weather correction, including the correction of CO_2.[41–46]

Oscillatory Rheological Measurements. The MCR 301 Anton Paar rheometer with a plate diameter of 25 mm operating in the cone and plate configurations under the oscillatory shear mode with a frequency $\omega = 10$ rad s^{-1} and a strain of 2% was used in the rheological investigations. A maximum cooling rate of 20°C min^{-1} was reached. Each experiment consisted of similar steps: first, the sample was melted at the initial temperature of 230°C and held at this temperature for 10 min to erase memories of previous processing as well as to reduce the normal stress that occurs during sample preparation. Afterward, the sample was cooled to the final temperature of 100°C at a constant cooling rate ϕ. Four different cooling rates, $\phi = 2.5$, 5, 10, and 20°C min^{-1}, were used, and the crystallization process was examined using the oscillatory shear mode.[47–52]

Wide-Angle X-ray Diffraction (WAXS). Wide-angle X-ray diffraction (WAXS) measurements were carried out by using a

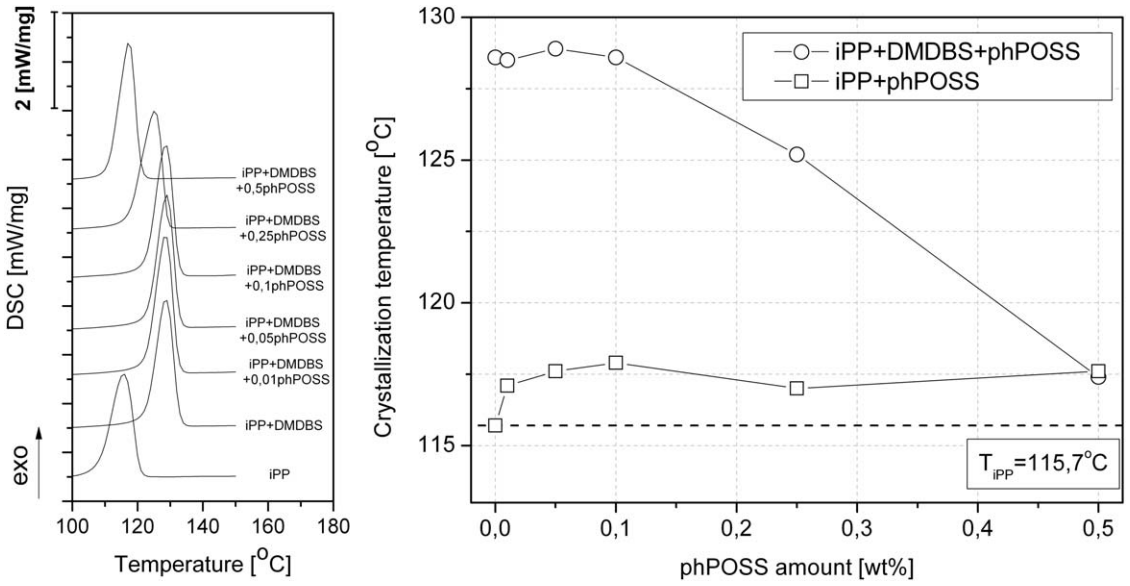

Figure 3. DSC crystallization curves and the crystallization temperature vs. the phPOSS content in DMDBS-nucleated iPP.

Seifert URD 6 aparatus. A monochromatic X-ray radiation with a wavelength of $\lambda = 1{,}5406$ Å (Cu Kα) was used. Identification was based on a reflected X-ray peak intensity analysis at a defined 2θ angle.[24] The evaluation of crystalinity degree measured by WAXS ($X_{C\text{-}WAXS}$) was performed with accordance to two-phase concept.[53,54] The crystallinity of each sample was obtained by analyzing the area under a crystallization peak and the complete area under diffraction curve. As suggested by Lima et al.,[53] in order to separate the crystalline fraction from the amorphous halo, the Gauss functions with a nonlinear regression program was used.

RESULTS AND DISCUSSION

Differential Scanning Calorimetry (DSC)

Calorimetric investigations were used to determine the effect of phPOSS addition to the DMDBS-nucleated iPP matrix. During the preliminary tests, a considerable decrease in the crystallization temperature (T_{cr}) was observed with increasing amount of phPOSS. For the maximum phPOSS concentration (0.5 wt %), a significant suppression of the nucleation effect was observed. The changes in T_{cr} as a function of phPOSS concentration, without a presence of nucleating agent, are presented in Figure 3. As it was previously observed in our former studies[55] the addition of POSS itself, in amounts lower than 1%, does not influence the crystallization behavior of isotactic polypropylene.

As shown in Figure 3, the addition of 0.25 wt % of DMDBS leads to an increase in the crystallization temperature to ~128°C, compared with the 115.7°C crystallization temperature of pure iPP. The introduction of a small amount of phPOSS (0.01–0.1 wt %) did not induce any changes in the iPP crystallization temperature. However, a higher than ~0.1 wt % amount of phPOSS induced a significant decrease in T_{cr} in comparison with the T_{cr} of the nucleated iPP/DMDBS blends. For the iPP samples that contained 0.5 wt % of phPOSS, a crystallization temperature similar to that of neat iPP was observed.

Thus, the samples that contain 0.25 wt % of phPOSS may attract interest for changing the parameters of the molten state processing of iPP.

Wide-Angle X-ray Diffraction (WAXS)

Figure 4 presents WAXS diffractograms of pure iPP, iPP nucleated with DMDBS and iPP nucleated with DMDBS and modified with various phPOSS amounts, registered at a room temperature. In all considered samples α-crystalline formation occurred and no evidence of the β-crystalline modification was observed. The characteristic reflections at folowing angles of 2θ (14.2, 17.0, 18.8, 21.2, and 22.0), corresponding to the crystalline planes (110), (040), (130), (111), and (041) respectively, were clearly visible.[24,53,54] No additional reflections at 16.2 and

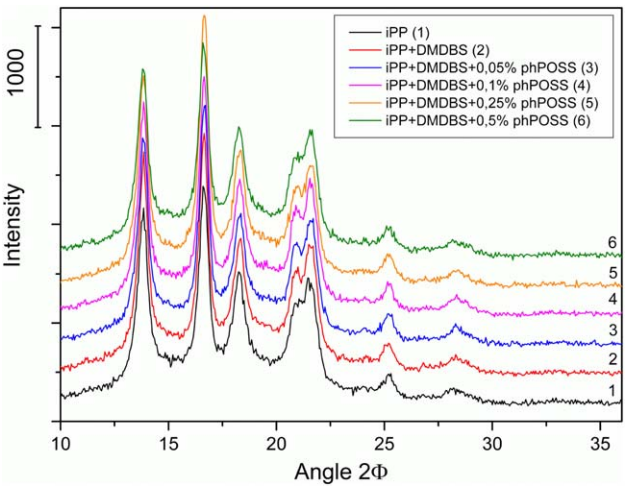

Figure 4. WAXS diffractograms carried out at a room temperature for iPP, nucleated iPP and nucleated iPP modified with phPOSS. [Color figure can be viewed in the online issue, which is available at wileyonlinelibrary.com.]

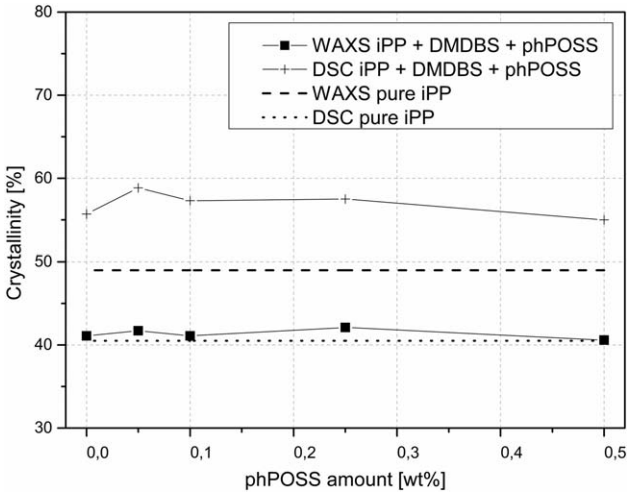

Figure 5. Crystallinity degree discrepancies between iPP, nucleated iPP and nucleated iPP modified with phPOSS samples obtained from DSC and WAXS measurements.

19.8 corresponding to β or γ iPP crystalline forms were observed as it was in former studies.[2] Therefore, it can be stated that modification of DMDBS by phPOSS led only to changes in crystallization behavior. What is more, no occurrence of polymorphism in polymer matrix was observed.

Crystallinity Determination by DSC and X-Ray Diffraction Methods

Two different techniques of crystallinity degree calculation were used. The results have been depicted in Figure 5. Discrepancy in samples' crystallinity degrees measured by WAXS in comparison to those obtained from DSC is probably caused by the thermomechanical history of the pressed specimens used for X-ray diffraction measurements. However, it should be noticed that in both cases a similar tendency could be observed. The highest amount of phPOSS led to a decrease of crystallinity degree of modified iPP. It is important to outline that the authors paid special attention to the material properties and not to the influence of pressure exerted on the material. That is why the crystallinity degrees calculated from the DSC measurements were the most accurate in this case.

Fourier Transform Infrared Spectroscopy (FTIR)

The possibility of different bond creations between the DMDBS and phPOSS particles was investigated using the FTIR method. It is known that even a small amount of phPOSS interferes with fibrillar network formation. This effect leads to the suggestion that the phPOSS particles interpose the favored fibrillar network formation, which is supposed to be maintained by the formation of hydrogen bonds between the —OH groups in DMDBS.[18,20] The FTIR spectra are presented in Figures 6 and 7.

The FTIR spectra of the sample that contained neat DMDBS were analyzed. An O—H stretching peak was observed at wavenumbers of 3427 and 3286 cm^{-1}. The O—H group was linked with intermolecular hydrogen bond, and what is more, the compound contained one hydrogen bridge. Furthermore, peaks from CH_2 and CH_3 groups appeared at ~2900 cm^{-1}. A separate peak at 1247 cm^{-1} was observed and assigned to the C—O stretching group.

Next, the FTIR spectra of the sample that contained phPOSS were examined. A peak was observed at a wavenumber of 3253 cm^{-1} due to associated O—H stretching. The O—H group was linked with intramolecular hydrogen bond, and what is more, the compound contained one hydrogen bridge. Moreover, aromatic C—H stretching was detected at several wavenumbers: 3074, 3053, and 3029 cm^{-1}. A cluster of peaks were spotted between 1595 and 1431 cm^{-1} and arose from aromatic C—C stretching. A strong peak at 1135 cm^{-1}, originating from silanol groups (Si—O), was observed. At the wavenumbers 744 and 697 cm^{-1}, aromatic C—H bending was observed. In the heated samples, the O—H peak appeared at a higher wavenumber and became wider. This proves weakening of the hydrogen bonds together with an increase of a temperature.

In the case of the mixtures that contained DMDBS and phPOSS and were heated to 190 and 287°C, the O—H peak location

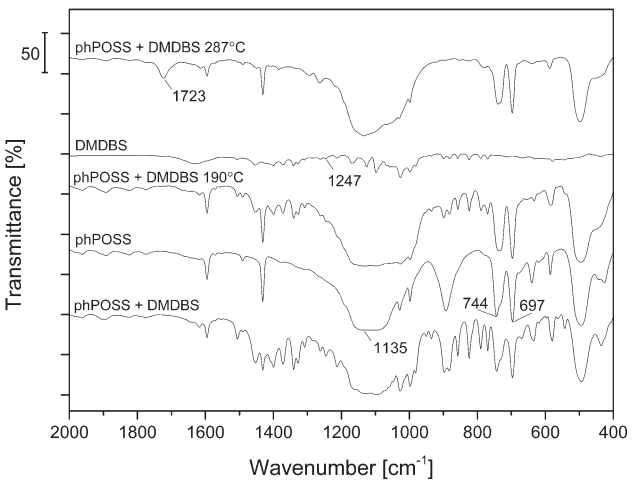

Figure 6. Transmittance vs. wavenumber FTIR spectra for various phPOSS and DMDBS compositions in a range from 400 to 2000.

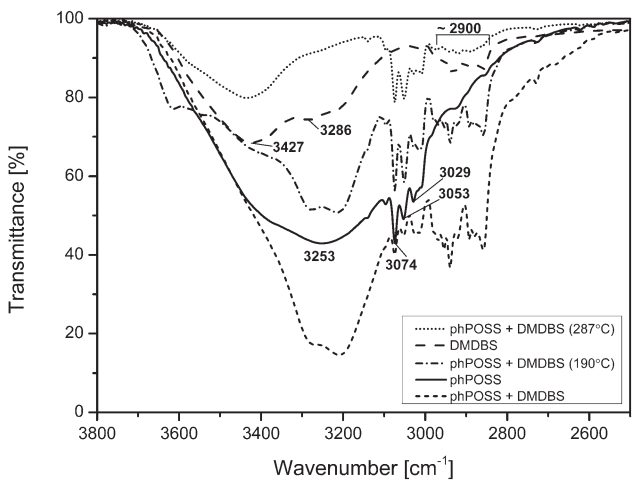

Figure 7. Transmittance vs. wavenumber FTIR spectra for various phPOSS and DMDBS compositions in a range from 2500 to 3800.

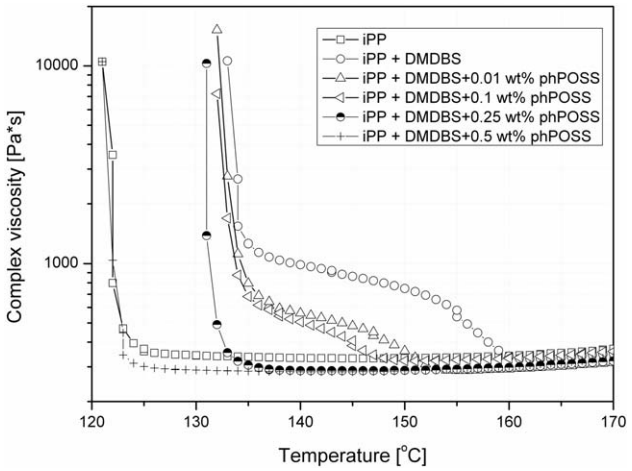

Figure 8. Complex viscosity curves vs. temperature obtained during the cooling of nucleated iPP modified with different amounts of phPOSS ($\phi = 10°C\ min^{-1}$).

shifted to higher wavenumbers. This result indicates the considerable weakening of the hydrogen bonds between the DMDBS particles and consequently the overlap of the interactions between the DMDBS and phPOSS molecules. Thus, an interaction occurs between the DMDBS and phPOSS molecules. The maximum temperature of the heated sample was 287°C. This was very close to the degradation temperature of phPOSS, and the compound began to decompose, as evidenced by the occurrence of the C═O stretch at a wavenumber of 1723 cm^{-1}. Moreover, the disappearance of the group of peaks at ~2900 cm^{-1} revealed a decay in the C—H groups. Nonetheless, the processing temperature used to produce specimens was much lower and equal to 190°C. The examination of the mixture at a temperature of 190°C proved that the overlap of the interactions between the DMDBS and phPOSS molecules was well-established by the O—H peak location shifted to higher wavenumber. What is even more essential, there was no evidence of the C═O stretch occurrence at a wavenumber of 1723 cm^{-1}. This observation confirmed that the process performed at 190°C led the DMDBS and phPOSS molecules interact without any degradation.

Following Roy et al.[20] a creation of hydrogen bond, that is an example of noncovalent interplay, may cause such a complex formation between POSS and DMDBS molecules. As a result, additives are able to form several elaborate molecular adducts. All of the above led to an interference in DMDBS fibrillation. It is important to point out that the phenomenon mentioned above proved a molecular complex formation between POSS and alcoholic O—H groups in DMDBS.

Crystallization under Shearing Conditions

Oscillatory rheological investigations were conducted during cooling processes to evaluate the effect of the interaction between different amounts of DMDBS and phPOSS on viscosity changes under shearing conditions (Figure 8).

The differences between nucleated and non-nucleated PP are significant in terms of the crystallization behavior. In the case of the nucleated iPP sample, the onset of dynamic viscosity appeared earlier during cooling and increased due to the fibrillar network formation of DMDBS. In contrast, an increasing phPOSS content led to a decrease in the viscosity growth that was caused by DMDBS nucleation effect. In the case of the addition of 0.5 wt % of phPOSS, an overall suppression of primary DMDBS activity was observed. Looking at the samples that contained 0.25 wt % of phPOSS, a different crystallization behavior was observed. Despite the fact that the interaction between phPOSS and DMDBS led to the removal of an early onset viscosity increase, the nucleation efficiency was only slightly reduced. The results that were obtained from the oscillatory rheological tests are in a good agreement with those that were obtained from the DSC investigations. Thus, 0.25 wt % of phPOSS is a sufficient quantity to modify the processing of nucleated PP significantly during cast film forming due to the shift in T_{cr} toward a lower temperature, which could lead to a high transparency extruded film due to the DMDBS addition.

To determine the role of the cooling conditions on the crystallization of the iPP/DMDBS/0.25 wt % phPOSS blends using the

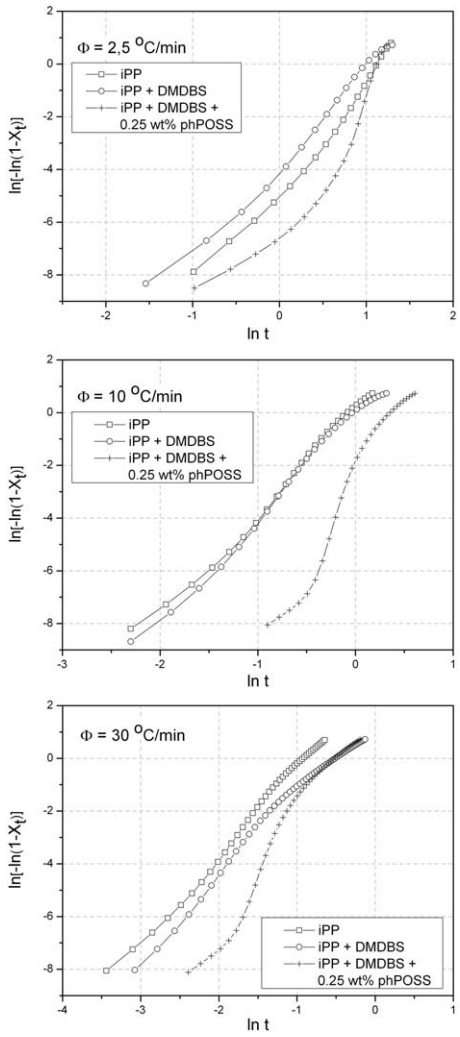

Figure 9. $\ln[-\ln(1 - X_t)]$ vs. $\ln t$ plots for pure iPP, nucleated iPP and nucleated iPP modified with phPOSS for three cooling rates: $\phi = 2.5$, 10, and 30°C min^{-1}.

Table I. Crystallization Parameters Obtained from the Avrami Analysis in Accordance with Jeziorny's Method

Sample	R	n	$\overline{n}$	Z_t	Z_c	R^2	$\overline{R^2}$	$t_{1/2}$
iPP	2.5	3.958	3.877	0.009	0.1490.602	0.979	0.989	3.022
	5	4.175		0.079	1.021	0.990		1.682
	10	3.954		1.228	1.096	0.991		0.865
	20	3.925		6.252	1.108	0.992		0.571
	30	3.373		21.823		0.994		0.359
iPP + DMDBS	2.5	3.489	3.738	0.024	0.226	0.987	0.987	2.612
	5	4.89		0.062	0.574	0.993		1.636
	10	3.935		0.956	0.995	0.990		0.921
	20	3.457		5.243	1.086	0.984		0.557
	30	2.919		4.576	1.052	0.979		0.524
iPP + DMDBS + 0.25 wt % phPOSS	2.5	4.352	5.373	0.002	0.090	0.887	0.953	3.657
	5	7.003		0.028	0.489	0.979		1.581
	10	6.817		0.076	0.773	0.964		1.382
	20	4.271		6.712	1.100	0.974		0.585
	30	4.242		9.884	1.079	0.963		0.548

oscillatory rheological investigations, measurements were conducted for various cooling rates from the molten state. Generally, the cooling rate had a considerable influence on the crystallization behavior, i.e., an earlier viscosity increase. The analysis of these crystallization effects, which are particularly vital for determining the possibility of a molten state draw to produce highly oriented products, will be published elsewhere.[56]

Non-Isothermal Crystallization Kinetics Analysis Using Avrami Theories Modified by Jeziorny

As mentioned above, the information regarding nucleation-induced crystallization leading to a viscosity increase at higher temperatures is especially important for the production of highly oriented materials. A significant limitation on the molten state draw ratio may arise from an early viscosity increase. To describe the crystallization of nucleated iPP in the presence of a phPOSS content higher than 0.25% quantitatively, a non-isothermal crystallization kinetics analysis was performed using the Avrami evaluation procedure described earlier in this article. The analysis was conducted for samples containing 0.25 wt % of phPOSS and 0.25 wt % of DMDBS. The $\ln[-\ln(1-X_t)]$ versus $\ln t$ curves for the pure iPP sample, the sample nucleated by DMDBS and the sample nucleated by DMDBS that was modified with phPOSS are presented in Figure 9.

In the graphs (Figure 9) of the $\ln[-\ln(1-X_t)]$ versus $\ln t$ plots, a similar crystallization behavior can be observed for the considered samples. The curves that represent the crystallization growth of the nucleated samples at a low cooling rate ($\phi = 2.5°C\ min^{-1}$) are shifted to a shorter crystallization time in comparison with the corresponding curves of the pure iPP samples. The growing fibrillar network of the sorbitol derivatives,[57] which leads to an increase in the crystallization rate, causes a decrease in the crystallization time and an increase in the crystallization temperature. It can be observed that the curve for the nucleated iPP sample (in comparison with the non-nucleated sample) changes its position when the cooling temperature is increased.

It is known[29] that the nucleation efficiency in the presence of DMDBS depends on the cooling conditions. The sample modified with 0.25 wt % of phPOSS revealed a different behavior; in the early stage, the crystallization process was highly suppressed. This result corresponds to the significant limitation of the fibrillar network growth during the primary crystallization stage. Note that the observed suppression effect of the nucleation efficiency is only slightly influenced by the cooling rate. This information may be helpful, particularly in the case of cast film production, when technological parameters, such as the temperature of chill rolls, need to be adjusted.

To describe the differences in crystallization behavior of all samples the approximate $\ln[-\ln(1-X_t)]$ curves were analyzed. Table I contained the crystallization parameters for the samples that were obtained from non-isothermal crystallization at different cooling rates in accordance with Jeziorny's method.

In our studies, the correlation coefficient R^2 of the approximate linearized Avrami plot was additionally analyzed (Table I). Within the considered range, pure and nucleated samples revealed a good linearity with the fitted curves ($R^2 = 0.99$ in both cases). A significant deviation of the averaged correlation coefficient in case of phPOSS modified samples (0.95) indicated that the changes in crystallization process resulted from more complex crystallization kinetics in comparison with nucleated iPP sample.

The Avrami exponent n and the parameters Z_t and Z_c can be evaluated once the approximation function for eq. (3) is assigned. It should be emphasized that the crystallization parameters n and Z_t considered in case of non-isothermal crystallization did not have the same physical meaning as in

isothermal crystallization. This was due to constantly lowering temperature during non-isothermal crystallization.[27,32,33] Following Piorkowska et al.,[30] taking these parameters into account would not result in a clear explanation due to a lack of their clear meaning.

The analysis of the crystallization constant Z_c values, which was a corrected kinetic rate constant and involved both nucleation and growth rate parameters, facilitated the evaluation of nucleation suppression effect caused by phPOSS. At lower cooling rates, i.e. up to 10°C min^{-1}, the values of Z_c for the samples that contained phPOSS were much lower than for pure or nucleated iPP. An increase of cooling rate limited a spherulites growth which narrowed differences between pure, nucleated and nucleated and modified iPP. However, it should be noticed that iPP modified with phPOSS was the least susceptible to cooling conditions. Furthermore, at higher cooling rates the Z_c values of phPOSS modified samples became similar to those obtained for nonmodified ones. In case of the highest cooling rate (30°C min^{-1}) the tendency in the value to fall was observed for nucleated samples. These results were in a good agreement to those presented in our previous studies.[56]

The crystallization halftime $t_{1/2}$ calculated as per eq. (6) allowed to describe the nucleation efficiency. For all considered samples the values of $t_{1/2}$ decreased with increasing cooling rate. However, an increase in the crystallziation rate, caused by the heterogenous nucleation, was perceived as a crystallization half time shortening. Therefore, the $t_{1/2}$ values observed for nucleated samples were slightly lower than those obtained from pure iPP. Crystallization behavior of phPOSS modified samples allowed to state that in case of low cooling rates (10°C min^{-1}) the nucleation effect caused by the presence of DMDBS is strongly suppressed.

The simultaneously analyzed values of the crystallization parameters Z_c, $t_{1/2}$ enabled to confirm the suppression of DMDBS nucleation effect on iPP caused by phPOSS modification.

It is worth mentioning that analysis of the Avrami exponent averages was conducted. The average values of n for pure, nucleated iPP and phPOSS modified samples were equal to 3.88; 3.73; and 5.37, correspondingly. As the first two values were close to 4 the process of thermal nucleation and three-dimensional spherical growth could occur in such case.[58] For all considered cooling rates of phPOSS modified samples, these values were significantly higher than for pure and nucleated iPP. This phenomenon indicated that the nucleation process of phPOSS modified samples was much more complex.

From an application point of view, an inhibition of DMDBS network formation delays an increase of viscosity in polymer melt. This in turn, may contribute to an elongation of time that is required when forming highly oriented goods.

The statement presented above is in a good agreement with these presented in our previous works.[59,60] It was indicated that the addition of phPOSS enables only a partial suspension of DMDBS activity as a clarifying effect and in the same time delays a viscosity increase. It was proved that phPOSS enables the production of highly oriented goods in the form of iPP fibers and moldings. In comparison to a nucleated matrix, a higher stretching degree, orientation and a lack of significant reduction of a clarifying effect were revealed.

CONCLUSIONS

As a result of iPP modification by DMDBS and by DMDBS modified with phPOSS via heterogeneous nucleation, various polymer crystallization behaviors were observed. It was demonstrated that different bonds between the DMDBS and phPOSS particles may be formed, leading to several changes in the crystal structure of the nucleated polymeric matrix.

The DSC analysis enabled the selection of an optimal concentration of phPOSS (0.25 wt %), leading to a lower nucleating agent efficiency.

The thermorheological results that were obtained during crystallization under shearing conditions indicated no significant influence of the cooling rate on the crystallization behavior of the nucleated iPP that was modified by 0.25 wt% of phPOSS. In this case, the early onset of viscosity, which may be the main restriction in the production of highly oriented products, was not observed.

The non-isothermal crystallization kinetics was examined using the Avrami theory that was modified by Jeziorny. A certain suppression effect of the crystallization efficiency was observed during the crystallization of phPOSS modified nucleated PP. On top of that it was also confirmed by the longer crystallization halftimes and lower values of Z_c crystallization parameters. However, it seemed that the modification efficiency could be strongly limited by too high cooling rates used.

From the application perspective, an interesting effect was established, i.e., a very low amount of silsesquioxanes is needed to achieve a controlled iPP crystallization behavior. Considering the relatively high price of silsesquioxanes, a low modifier quantity is vital for economic reasons.

ACKNOWLEDGMENTS

The study was conducted under Development Project POIG 01.03.01-30-173/09 Nanosil from the European Regional Development Fund within the Innovative Economy Operational Programme. The authors are grateful to Milliken & Company for supplying the nucleating agent samples for research.

REFERENCES

1. Fina, A.; Tabuani, D.; Camino, G. *Eur. Polym. J.* **2010**, *46*, 14.
2. Fina, A.; Tabuani, D.; Frache A.; Camino, G. *Polymer* **2005**, *46*, 7522.
3. Fina, A.; Abbenhuis, H. C. L.; Tabuani, D.; Frache, A.; Camino, G. *Polym. Degrad. Stab.* **2006**, *91*, 1064.
4. Maciejewski, H.; Dutkiewicz, M.; Byczyński, Ł.; Marciniec, B. *Polimery* **2012**, *57*, 535.
5. Zhou, Z.; Zhang, Y.; Zhang, Y.; Yin, N. *J. Polym. Sci. B Polym. Phys.* **2007**, *46*, 526.

6. Chen, J. H.; Chiou, Y. D. *J. Polym. Sci. B Polym. Phys.* **2006**, *44*, 2122.
7. Zhou, Z.; Cui, L.; Zhang, Y.; Zhang, Y.; Yin, N. *J. Polym. Sci. B Polym. Phys.* **2008**, *46*, 1762.
8. Janowski, B.; Pielichowski, K. *Polimery* **2008**, *53*, 85.
9. Andrzejewska, E.; Marcinkowska, A.; Prządka, D.; Kloziński, A.; Jakubowska, P. *Polimery* **2013**, *58*, 794.
10. Czarnecka-Komorowska, D.; Sterzynski, T.; Maciejewski, H.; Dutkiewicz, M.; *Compos. Theory Practice* **2012**, *12*, 232.
11. Fu, B. X; Yang, L.; Somani, R. H.; Zong, S. X.; Hsiao, B. S.; Phillips, S.; Blansky, R.; Ruth, P. *J. Polym. Sci. B Polym. Phys.* **2001**, *39*, 2727.
12. Zhou, Z.; Cui, L.; Zhang, Y.; Zhang, Y.; Yin, N. *Eur. Polym. J.* **2008**, *44*, 3057.
13. Lin, O. H.; MohdIshak, Z. A.; MdAkil, H. *Mater. Des.* **2009**, *30*, 748.
14. Choi, J. H.; Jung, C. H.; Kim, D. K.; Suh, D. H.; Nho, Y. C.; Kang, P. H.; Ganesan, R. *Radiat. Phys. Chem.* **2009**, *78*, 517.
15. Ambrożewicz, D.; Marciniec, B.; Jesionowski, T. *Chem. Eng. J.* **2012**, *210*, 229.
16. Perrin, F. X.; Bruzaud, S.; Grohens, Y. *Appl. Clay Sci.* **2010**, *49*, 113.
17. Zhao, F.; Bai, X.; McLauchlin, A. R.; Gu, J.; Wan, C.; Kandasubramanian, B. *Appl. Clay Sci.* **2010**, *47*, 249.
18. Roy, S.; Byoung, J. L.; Zahi, M. K.; Sadhan, C. *J. Macromolecules* **2012**, *45*, 2420.
19. Roy, S.; Sadhan, J. *Antec Conference Proc.* **2011**, *69*, 1105.
20. Roy, S.; Scionti, V.; Jana, S. C.; Wesdemiotis, C.; Pischera, A. M.; Espe, M. P. *Macromolecules* **2011**, *44*, 8064.
21. Lotz, B.; Wittmann, J. C.; Lovinger, A. *J. Polymer* **1996**, *37*, 4979.
22. Varga, J. *J. Macromol. Sci. Phys. B* **2002**, *41B*, 1121.
23. Gahleitner, M.; Grein, C.; Kheirandish, S.; Wolfschwenger, J. *Int. Polym. Proc.* **2011**, *26*, 2.
24. Romankiewicz, A.; Sterzyński, T.; Brostow, W. *Polym. Int.* **2004**, *53*, 2086.
25. Yoshida, K.; Morimoto, Y.; Watanabe, K.; Otake, N.; Inagaki, J.; Ohguma, K. *WO* 2003024870 A1.
26. Otake, N.; Yoshida, K. *JP* 2006182650.
27. Di Lorenzo, M. L.; Silvestre, C. *Prog. Polym. Sci.* **1999**, *24*, 917.
28. Paukszta, D.; Borysiak, S.; *Polimery* **2009**, *54*, 126.
29. Zhang, Y.; Li, X.; Wei, X. *J. Therm. Anal. Calorim.* **2010**, *100*, 661.
30. Piorkowska, E.; Galeski, A.; Haudin, J.-M. *Prog. Polym. Sci.* **2006**, *31*, 549.
31. Wu, H.; Liang, M.; Lu, C. *Thermochim. Acta*, **2012**, *545*, 148.
32. Liu, H.; Yang, G.; He, A.; Wu, M. *J. Appl. Polym. Sci.* **2004**, *94*, 819.
33. Liu, P.; Hu, A.; Wang, S.; Shi, M.; Ye, G.; Xu, J. *J. Appl. Polym. Sci.* **2011**, *121*, 14.
34. Ma, Y.; Hu, G.; Ren, X.; Wang, B. *Mater. Sci. Eng. A.* **2007**, 460/461, 611.
35. Kelar, K.; Olejniczak, J.; Barczewski, M. *Przem. Chem.* **2013**, *92*, 1000.
36. Apiwanthanakorn, N.; Supaphol, P.; Nithitanakul, M. *Polym. Test* **2004**, *23*, 817.
37. Duan, Q.; Wang, B.; Hong, B.; Wang, H. *J. Macromol. Sci. B Phys.* **2010**, *49*, 1094.
38. Liu, M.; Zhao, Q.; Wang, Y.; Zhang, C.; Mo, Z.; Cao, S. *Polymer* **2003**, *44*, 2537.
39. Jin, J.; Chen, S. J.; Zhang, J. *eXPRESS Polymer Lett* **2010**, *4*, 141.
40. Sui, G.; Zhong, W.-H.; Fuqua, M. A.; Ulven, C.A. *Macromol. Chem. Phys.* **2007**, *208*, 1928.
41. Wan, C.; Zhao, F.; Bao, X.; Kandasubramanian, B.; Duggan, M. *J. Polym. Sci. B Polym. Phys.* **2009**, *47*, 121.
42. Sevegney, M. S.; Kannan, R. M.; Siedle, A. R.; Percha, A. *J. Polym. Sci. B Polym. Phys.* **2005**, *43*, 439.
43. Verker, R.; Grossman, E.; Gouzman, I.; Eliaz, N. *Compos. Sci. Technol.* **2009**, *69*, 2178.
44. Ojeda, T.; Liberman, S.; Amorim, R.; Samios, D. *J. Polym. Eng.* **2011**, *16*, 105.
45. Weihua, L.; Jingyuan, W.; Yaoxian, L.; Yuwei, L.; Xinyi, T. *J. Polym. Eng.* **2011**, *15*, 271.
46. Kelar, K.; Jurkowski, B.; Mencel, K. *Polimery* **2005**, *6*, 449.
47. Khanna, Y. P. *Macromolecules* **1993**, *26*, 3639.
48. Eder, G.; Janeschitz-Kriegl, H. *Colloid Polym. Sci.* **1988**, *266*, 1087.
49. Pantani, R.; Coccorullo, I.; Volpe, V.; Titomanlio, G. *Macromolecules* **2010**, *43*, 9030.
50. Sun, T.; Chen, F.; Dong, X.; Zhou, Y.; Wang, D.; Han, C. C. *Polymer* **2009**, *50*, 2465.
51. Xu, Z.; Sun, N.; Li, H. *J. Polym. Eng.* **2012**, *32*, 153.
52. Bouhelal, S.; Cagiao, M. E.; Di Lorenzo, M. L.; Zouai, F.; Khellaf, S.; Tabet, H.; Benachour, D.; Calleja, F. J. B. *J. Polym. Eng.* **2012**, *32*, 143.
53. Lima, M. F. S.; Vasconellos, M. A. Z.; Samios D. *J. Polym. Sci. B Polym. Phys.* **2002**, *40*, 896.
54. Chen, Y.-H.; Mao, Y.-M.; Li, Z.-M.; Hsiao, B. S. *Macromolecules* **2010**, *43*, 6760.
55. Barczewski, M.; Czarnecka-Komorowska, D.; Andrzejewski, J.; Sterzyński, T.; Dutkiewicz, M.; Dudziec, B. *Polimery* **2013**, *10*, 805.
56. Dobrzyńska-Mizera, M.; Barczewski, M.; Dudziec, B.; Sterzyński, T. *Polimery* **2013**, *58*, 88.
57. Wilder, E. A.; Hall, C. K.; Khan, S. A.; Spontak, R. *J. Langmuir* **2003**, *19*, 6004.
58. Duan, J.; Dou, Q. *J. Appl. Polym. Sci.* **2013**, *130*, 206.
59. Barczewski, M.; Chmielewska, D.; Sterzyński, T.; Andrzejewski, J. *Polym. Process.* **2012**, *149*, 409.
60. Barczewski, M.; Dobrzyńska-Mizera, M.; Andrzejewski, J.; Chmielewska, D. *Polym. Process.* **2013**, *153*, 139.